PHYSICAL REVIEW LETTERS

Density Profiles of Strongly Interacting Trapped Fermi Gases

Jelena Stajic,* Qijin Chen, and K. Levin

James Franck Institute and Department of Physics, University of Chicago, Chicago, Illinois 60637, USA
(Received 4 August 2004; revised manuscript received 10 November 2004; published 14 February 2005)

We study density profiles in trapped fermionic gases, near Feshbach resonances, at all $T \leq T_c$ and in the near Bose-Einstein condensation and unitary regimes. For the latter, we characterize and quantify the generally neglected contribution from noncondensed Cooper pairs. As a consequence of these pairs, our profiles are rather well fit to a Thomas-Fermi (TF) functional form, and equally well fit to experimental data. Our work lends support to the notion that TF fits can be used in an experimental context to obtain information about the temperature.

There is now strong, but not unambiguous, evidence that fermionic superfluidity has been observed [1−6] in trapped atomic gases where the strength of the pairing interaction can be arbitrarily tuned via Feshbach resonance effects. Experimental proof of superfluidity is not straightforward, except in the Bose-Einstein condensation (BEC) regime where the particle density profiles provide evidence for a condensation via their bi-modal form [7]. Intermediate between the BCS and BEC regimes, the measured density profiles [8,9] in traps do not contain any obvious signatures of superfluidity, although such features have been predicted theoretically [10,11].

The goals of this Letter are to compute the particle density profiles at all $T \leq T_c$ (where T_c is the superfluid transition temperature) in the near-BEC and unitary regimes in order to reconcile theory and experiment. For the former our calculation of the contribution from noncondensed bosons leads to important corrections to estimates of the condensate fraction based on the conventional Gaussian form. For the unitary case, these noncondensed pairs smooth out the otherwise abrupt transition between the condensate and the thermal background of fermionic excitations; this explains why the measured density profiles appear to be so featureless [8,9].

The unitary or strongly interacting Fermi gas has been the focus of attention by the community. Some time ago it was found [8] that the profiles were reasonably well described by a Thomas-Fermi (TF) functional form at zero T, and in recent work [12] this procedure has been extended to finite temperatures. Below T_c all previous theoretical work (which either ignored noncondensed pair states [10,11] or used a different ground state [13]) has predicted strong deviations from this T-dependent TF functional form. It is extremely important, thus, to have a better understanding of the spatial profiles. Our work lends theoretical support to the viewpoint [12] that TF fits (with proper calibration) can be used in an experimental context to obtain information about the temperature. In addition to establishing these TF fits to theory, we compare theory and experiment directly via one-dimensional representations of their respective profiles. We demonstrate remarkable agreement in the shapes of the two profiles. One can infer from this comparison experimental support, albeit indirect, for the presence of a superfluid condensate.

The first generation theories [14] have focused on a BCS-like ground state [15] which is readily generalized to accommodate a "two-channel" variant [16] in which Feshbach bosonic (FB) degrees of freedom are present as well. This approach has met with some initial success in addressing collective mode experiments [17,18] and pairing-gap spectroscopy [19]. The excitations of this standard ground state [14,16] consist of two types: noncondensed fermion pairs hybridized with FB and Bogoliubov-like fermionic excitations having $E_{\mathbf{k}} \equiv \sqrt{(\epsilon_{\mathbf{k}} - \mu)^2 + \Delta^2(T)}$, where $\epsilon_{\mathbf{k}}$ is the free fermion kinetic energy. Note that the "gap parameter" $\Delta(T)$ is in general different from the superconducting order parameter, $\tilde{\Delta}_{\mathrm{sc}}$. Recent rf experiments [5] have been analyzed [19] using our formalism to suggest that the quasiparticles have an energy gap or pseudogap, which is present well above T_c, and, thus, not directly related to the order parameter. Additional support for this "pseudogap" has recently been reported in another very different class of experiments [20].

We summarize the self-consistent equations [21] in the presence of a spherical trap, treated at the level of the local density approximation (LDA) with trap potential $V(r) = \frac{1}{2}m\omega^2 r^2$. T_c is defined as the highest temperature at which the self-consistent equations are satisfied precisely at the center. At $T < T_c$ the superfluid region extends to a finite radius R_{sc}. The particles outside this radius are in a normal state, with or without a pseudogap. Our self-consistent equations are given in terms of the Feshbach coupling constant g and interfermion attractive interaction U by a gap equation

$$1 + \left[U + \frac{g^2}{2\mu - 2V(r) - \nu} \right] \sum_{\mathbf{k}} \frac{1 - 2f(E_{\mathbf{k}})}{2E_{\mathbf{k}}} = 0, \quad (1)$$

which is imposed only when $\mu_{\mathrm{pair}}(r) = 0$. The pseudogap contribution to $\Delta^2(T) = \tilde{\Delta}_{\mathrm{sc}}^2(T) + \Delta_{\mathrm{pg}}^2(T)$ is given by

$$\Delta_{\text{pg}}^2 = \frac{1}{Z}\sum_{\mathbf{q}} b(\Omega_q - \mu_{\text{pair}}). \qquad (2)$$

Here $b(x)$ is the Bose function. The various residues, Z and Z_b, are described in Ref. [14]. The quantity $\Omega_{\mathbf{q}}$ is the pair dispersion, and μ_{pair} and μ_{boson} are the effective chemical potentials of the pairs and FB.

We introduce units $\hbar = 1$, fermion mass $m = \frac{1}{2}$, Fermi momentum $k_F = 1$, and Fermi energy $E_F = \hbar\omega(3N)^{1/3} = 1$. In the figures below, we express length in units of the Thomas-Fermi radius $R_{\text{TF}} = \sqrt{2E_F/(m\omega^2)} = 2(3N)^{1/3}/k_F$; the density $n(r)$ and total particle number $N = \int d^3\mathbf{r} n(r)$ are normalized by k_F^3 and $(k_F R_{\text{TF}})^3$, respectively. The local density can be written as

$$n(r) = 2n_b^0 + \frac{2}{Z_b}\sum_{\mathbf{q}} b(\Omega_q - \mu_{\text{boson}})$$
$$+ 2\sum_{\mathbf{k}}\{v_{\mathbf{k}}^2[1 - f(E_{\mathbf{k}})] + u_{\mathbf{k}}^2 f(E_{\mathbf{k}})\}, \qquad (3)$$

where $n_b^0 = g^2\tilde{\Delta}_{\text{sc}}^2/\{[\nu - 2\mu + 2V(r)]U + g^2\}^2$ is the molecular Bose condensate which is only present for $r \leq R_{\text{sc}}$. The chemical potential $\mu_{\text{pair}} = \mu_{\text{boson}}$ is identically zero in the superfluid region $r < R_{\text{sc}}$, and must be solved for self-consistently at larger radii. Our calculations proceed by solving numerically the self-consistent equations.

We now decompose the density profiles into components associated with the condensate, the noncondensed pairs and the fermions. This raises a central issue of this Letter. What is the most suitable definition of the condensate ratio in a fermionic superfluid? Indeed, in strict BCS theory there are two alternatives [22], one based on the superfluid density and the other based on associating the condensate with the perturbation of the superfluid state relative to the underlying *free* Fermi gas. In BCS theory with this second definition, the zero temperature condensate fraction is of order T_c/E_F, far from the value 100%, which one obtains from the superfluid density. Physically, this second definition reflects the fraction of the original Fermi liquid states which are modified substantially by
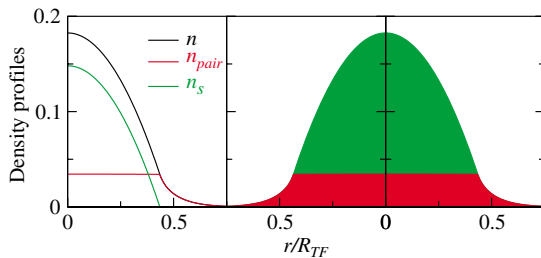

FIG. 1 (color online). Density profile and its decomposition in the near-BEC limit ($1/k_F a = 3.0$) at $T/T_c = 0.5$. Shown are the actual plots on the left for the total $n(r)$, the noncondensed pairs n_{pair}, and the condensate n_s. The right panel shows how these two (indicated by the shaded areas from top to bottom) add together to give $n(r)$.

pairing. We explore both of these here, since they are expected to enter in different physical contexts. In the BEC regime (where fermions are absent) there is no distinction between the two decompositions, and thus the condensate fraction is uniquely defined.

In the present approach to the BCS-BEC crossover picture it is relatively straightforward to deduce [14] the (local) superfluid density, $n_s \equiv n_s(r)$. For the one-channel model we find [14] a simple result for n_s, as well as for the fermionic quasiparticle (n_{QP}) and pair contributions (n_{pair}) to the difference $n - n_s$:

$$n_s = \frac{\tilde{\Delta}_{sc}^2}{\Delta^2} n_s^{\text{BCS}}(\Delta), \qquad (4a)$$

$$n_{\text{pair}} = \frac{\Delta_{pg}^2}{\Delta^2} n_s^{\text{BCS}}(\Delta) = n_s^{\text{BCS}}(\Delta) - n_s, \qquad (4b)$$

$$n_{\text{QP}} = n - n_s^{\text{BCS}}(\Delta), \qquad (4c)$$

where n_s^{BCS} is the usual superfluid density for a gas of fermions within BCS theory, except that here the full excitation gap Δ appears instead of the order parameter. In the one-channel case the order parameter $\tilde{\Delta}_{\text{sc}}$ is equal to the Cooper condensate contribution (which we call Δ_{sc}). For the broad Feshbach resonances of ^{40}K and ^{6}Li, these one-channel results are appropriate for the unitary and BCS regimes of the two-channel case. In the BEC regime ($\mu < 0$), the contribution of the fermionic quasiparticles becomes negligible. Therefore, Eqs. (4) reduce to

$$n_s = \frac{\tilde{\Delta}_{sc}^2}{\Delta^2} n, \qquad n_{\text{pair}} = \frac{\Delta_{pg}^2}{\Delta^2} n. \qquad (5)$$

Interestingly, this result is also valid for the two-channel problem in the BEC regime.

Formally, we can address the second decomposition of the density profiles by writing the particle density in terms of the single particle Green's function $G(K) = G_0(K) + G_0(K)\Sigma(K)G(K)$, where G_0 represents free fermions and $K \equiv (i\omega_n, \mathbf{k})$ is the four momentum. The second term is then further split into the condensed ($\propto \tilde{\Delta}_{\text{sc}}^2$) and non-condensed ($\propto \Delta_{\text{pg}}^2$) components. Summing over the Matsubara frequencies ω_n and adding the FB contribution, one obtains

$$\tilde{n}_s = 2Z\tilde{\Delta}_{sc}^2, \qquad (6a)$$

$$\tilde{n}_{\text{pair}} = 2\sum_{\mathbf{q}\neq 0} b(\Omega_q - \mu_{\text{pair}}) = 2Z\Delta_{pg}^2, \qquad (6b)$$

$$\tilde{n}_{\text{ferm}}^{\text{free}} = 2\sum_{\mathbf{k}} f(\epsilon_{\mathbf{k}} - \mu + V(r)), \qquad (6c)$$

which correspond to condensate density, finite momentum pair/boson density, and free fermion density, respectively.

We characterize the crossover regime by the parameter $1/k_F a$ where a is the interatomic s-wave scattering length. A typical density profile for the near-BEC limit with $1/k_F a = 3.0$ is shown in Fig. 1 for $T/T_c = 0.5$. This plot is in the physically accessible near-BEC regime where the

bosons are still primarily Cooper pairs, as distinguished from Feshbach bosons. Based on experiments [3,4] and related theory [17,18] this is not yet in the deep BEC where the collective modes are expected to exhibit the characteristics of true bosons [23]. Thus one expects the ground state wave function to be applicable here. The left panel corresponds to actual plots of the condensed (green curve) and noncondensed pair contributions (red) while the shaded regions on the right represent from top to bottom the condensed (green) and noncondensed bosons (red), respectively. For this BEC plot, there are no fermions. Importantly, the contribution from the noncondensed bosons is essentially constant in r until R_{sc}, reflecting the fact that they have a gapless excitation spectrum ($\mu_{pair} = 0$). However, once μ_{pair} is nonzero at the trap edge the number of noncondensed bosons (n_{pair}) drops rapidly.

Figure 1 is consistent with the experimentally observed profile shapes [9], but it can be contrasted with other theoretical results in the literature which predict nonmonotonic features [13]. Because all direct interactions are via fermions, the character of the BEC profile is different from that of true interacting bosons. These differences also appear in the context of collective mode experiments [17,18,23]. As for true bosons [7,24], the constraint that the bosons are gapless in the superfluid region is important for determining their density distribution. A clear bi-modal feature or "kink" at R_{sc} is present and provides evidence for the existence of a condensate. It should be noted that the inferred fraction of the condensate may be significantly smaller than found here—if a Gaussian form is assumed throughout the trap (as is the experimental convention) for estimating the contribution from noncondensed pairs.

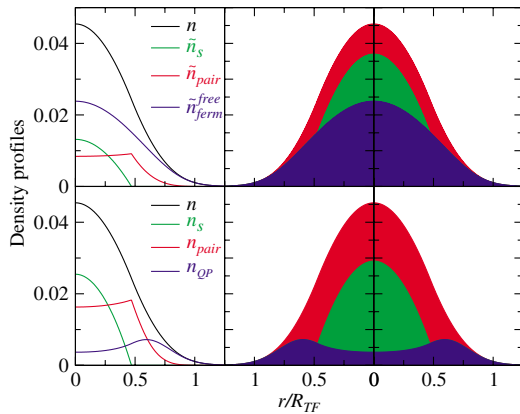In the upper and lower panels of Fig. 2 we plot the density distributions in the unitary limit, $1/k_F a = 0$, as a

FIG. 2 (color online). Density profiles and their decompositions for the unitary case ($1/k_F a = 0$) at $T = 0.75T_c$. The upper and lower panels correspond to Eqs. (6) and Eqs. (4), respectively. On the left are shown the actual plots for the total, the noncondensed pairs, condensate, and fermion density. Shown on the right is how the last three, as indicated by the shaded areas from top to bottom of each panel, add up to the local density $n(r)$.

function of radius r at $T/T_c = 0.75$, and show their different decompositions following Eqs. (6) and Eqs. (4), respectively. The superfluid-based decomposition (lower panels) appears to be more relevant to thermodynamics [12] and recent rf experiments [5,19] since it incorporates the excitation gap of the fermions. The decomposition in the upper panels, based on free fermions, was studied in detail in Ref. [13], for a somewhat different ground state.

The shaded regions on the right of each figure correspond (from top to bottom) to density profiles of noncondensed pairs, condensate, and fermionic quasiparticles. In both decompositions the noncondensed pairs play a significant role. It can be seen from the plots on the left of Fig. 2 that the noncondensed pairs show a relatively flat density distribution for $r \lesssim R_{sc}$, just as in the near-BEC limit of Fig. 1. This behavior similarly arises from the vanishing of $\mu_{pair}(r)$ in the superfluid region.

One can see that the condensate has substantially more weight for the n_s-based decomposition [Eq. (4), Fig. 2, lower panels]. Conversely the excited fermions for this case are significantly less important, since they experience a large gap in their excitation spectrum. The contribution of these fermions is concentrated at the trap edge. Indeed, for this case, the fermions and noncondensed bosons generally appear in different regions of the trap. The latter are associated with the regions where the gap is largest (and the fermions are quasibound into "bosonic"-like states), and the former are found where the gap is smallest.

In Fig. 3 we compare theory and experiment for the unitary case. The experimental data were estimated to correspond to roughly this same temperature ($T/T_F = 0.19$) based on the analysis of Ref. [12]. The profiles shown are well within the superfluid phase ($T_c \approx 0.3T_F$ at unitarity). This figure presents Thomas-Fermi fits [12] to the experimental [Fig. 3(a)] and theoretical [Fig. 3(b)] profiles as well as their comparison [Fig. 3(c)] for a chosen $R_{TF} = 100\ \mu m$, which makes it possible to overlay the experimental data (circles) and theoretical curve (line). Finally Fig. 3(d) indicates the relative χ^2 or root-mean-square (rms) deviations for these TF fits to theory. This figure was made in collaboration with the authors of Ref. [12]. Two of the three dimensions of the theoretical trap profiles were integrated out to obtain a one-dimensional representation of the density distribution along the transverse direction: $\bar{n}(x) \equiv \int dy dz\, n(r)$.

This figure is in contrast to earlier theoretical studies which predict a kink at the condensate edge [10,11]. Moreover, in contrast to the predictions of Ref. [13], the curves behave monotonically with both temperature and radius. Indeed, in the unitary regime the generalized TF fitting procedure of Ref. [12] works surprisingly well for our theory with spherical traps, and for anisotropic experiments [shown in Fig. 3(a)]. This is, in part, a consequence of the fact that trap anisotropy effects become irrelevant for these one-dimensional projections. These reasonable TF fits apply to essentially all temperatures investigated ex-
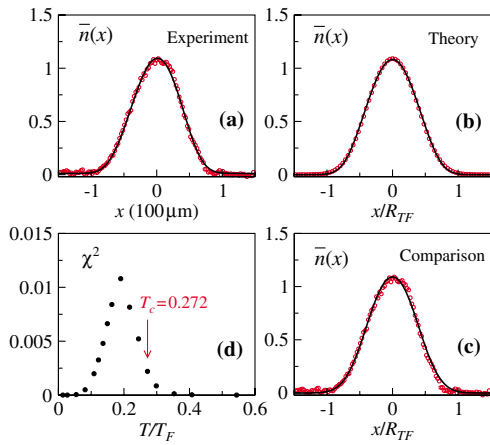
FIG. 3 (color online). Temperature dependence of (a) experimental one-dimensional spatial profiles (circles) and TF fit (line) from Ref. [12], (b) TF fits (line) to theory both at $T \approx 0.7T_c \approx 0.19T_F$ (circles), and (c) overlay of experimental (circles) and theoretical (line) profiles, as well as (d) relative rms deviations (χ^2) associated with these fits to theory at unitarity. The circles in (b) are shown as the line in (c). The profiles have been normalized so that $N = \int \bar{n}(x)dx = 1$, and we set $R_{\mathrm{TF}} = 100 \, \mu$m in order to overlay the two curves. χ^2 reaches a maximum around $T = 0.19T_F$.

perimentally [12] and all temperatures we have studied, including in the normal state.

To probe the deviations from a TF functional form, and to establish the role of the condensate, in Fig. 3(d), we show the (relative) rms deviation, or χ^2, from the TF fits as a function of T. Except at the very lowest temperatures (where the χ^2 is small and the condensate occupies the entire region of the trap), the condensate causes a small but potentially measurable variation from the TF form. χ^2 increases rapidly below T_c and reaches a maximum around $0.7T_c$. Here the profile involves two different functional forms: the condensate and the thermal distribution functions. More precisely, the systematic behavior of χ^2 indicates when T has safely surpassed T_c.

The reason the Thomas-Fermi fits work well below T_c has to do with the presence of noncondensed pairs. If these bosoniclike states are ignored (by omitting the topmost shaded regions), in the right panels of Fig. 2, a clear bimodal distribution emerges, as has been predicted in the literature [10,11]. In this case, TF fits would not work well. A residue of this bi-modality must be present in the present plots, but this can only be seen in the derivatives of our profiles. We find a small kink in the first order derivative and a sharp jump in the second order derivative of $n(r)$, reflecting the condensate edge. These features may be more difficult to identify with current experimental techniques. Alternatively, one may infer the presence of a condensate through χ^2 plots from TF fits. These experiments will require substantial averaging over a large number of profiles, however.

In summary, in this Letter we have found that, in the near-BEC regime, the component profile for the noncondensed bosons is different from the Gaussian form generally assumed, although the general shape is consistent with experiment. Near unitarity, we have found that our calculated density profiles are consistent with experiment and provide strong support for using Thomas-Fermi fits to the profiles. One can infer that the condensate is seen, not in the profile shapes, but, presumably, in their temperature calibration [12].

*Present address: Los Alamos National Laboratory, Los Alamos, NM 87545.
 [1] C. A. Regal, M. Greiner, and D. S. Jin, Phys. Rev. Lett. **92**, 040403 (2004).
 [2] M. W. Zwierlein *et al.*, Phys. Rev. Lett. **92**, 120403 (2004).
 [3] J. Kinast *et al.*, Phys. Rev. Lett. **92**, 150402 (2004).
 [4] M. Bartenstein *et al.*, Phys. Rev. Lett. **92**, 203201 (2004).
 [5] C. Chin *et al.*, Science **305**, 1128 (2004).
 [6] J. Kinast, A. Turlapov, and J. E. Thomas, Phys. Rev. A **70**, 051401 (2004).
 [7] F. Dalfovo *et al.*, Rev. Mod. Phys. **71**, 463 (1999).
 [8] K. M. O'Hara *et al.*, Science **298**, 2179 (2002).
 [9] M. Bartenstein *et al.*, Phys. Rev. Lett. **92**, 120401 (2004).
[10] T.-L. Ho, Phys. Rev. Lett. **92**, 090402 (2004).
[11] M. L. Chiofalo *et al.*, Phys. Rev. Lett. **88**, 090402 (2002).
[12] J. Kinast *et al.*, cond-mat/0502087 (Science, published online 27 January 2005).
[13] A. Perali *et al.*, Phys. Rev. Lett. **92**, 220404 (2004).
[14] Q. J. Chen, J. Stajic, S. N. Tan, and K. Levin, cond-mat/0404274.
[15] A. J. Leggett, in *Modern Trends in the Theory of Condensed Matter* (Springer-Verlag, Berlin, 1980), pp. 13–27.
[16] J. Stajic, Q. J. Chen, and K. Levin, Phys. Rev. A (to be published).
[17] H. Hu *et al.*, Phys. Rev. Lett. **93**, 190403 (2004).
[18] H. Heiselberg, Phys. Rev. Lett. **93**, 040402 (2004).
[19] J. Kinnunen *et al.*, Science **305**, 1131 (2004).
[20] M. Greiner, C. A. Regal, and D. S. Jin, Phys. Rev. Lett. (to be published).
[21] J. Stajic *et al.*, Phys. Rev. A **69**, 063610 (2004).
[22] A. J. Leggett, Talk at the KITP, UCSB, May, 2004 (unpublished).
[23] S. Stringari, Europhys. Lett. **65**, 749 (2004).
[24] H. Shi and A. Griffin, Phys. Rep. **304**, 1 (1998).